14th International Conference on Applications of Statistics and Probability in Civil Engineering, ICASP14
Dublin, Ireland, July 9-13, 2023

Stochastic approximation of fatigue damage for in-service monitoring of structures

Clément Freyssinet
Nantes Université, École Centrale Nantes, CNRS, GeM, UMR 6183, F-44000 Nantes, France

Valentine Rey
Nantes Université, École Centrale Nantes, CNRS, GeM, UMR 6183, F-44000 Nantes, France

Franck Schoefs
Nantes Université, École Centrale Nantes, CNRS, GeM, UMR 6183, F-44000 Nantes, France

Tanguy Moro
Nantes Université, IRT Jules Verne, F-44000 Nantes, France

ABSTRACT: In this paper, we focus on polycyclic fatigue of structures in a reliability context. First, we identify the random material parameters of the two-scale non linear cumulative damage fatigue model from S-N curves. Then, we compare linear and non linear cumulative damage on a plate for three loads. Finally, we propose to build a multi-fidelity meta-model to control computation costs of the estimation of the final probability of failure.

1. INTRODUCTION

Fatigue has a major impact on the lifetime of many industrial structures subjected to large repetition of low amplitude oscillating loads (offshore wind turbines or platforms, air crafts, train rails, ...). Unfortunately, the prediction of fatigue degradation is very difficult because uncertainties affect the loads and the material parameters. This is the reason why reliability-based design and assessment of structures are crucial to take into account those uncertainties. Linear damage accumulation (Miner (2021)) is a widespread approach to compute at low cost the fatigue damage evolution. The local stress at one hotspot (computed or measured thanks to monitoring) is decomposed thanks to Rainflow counting (Hong (1991)) and the Palmgreen and Miner's rule associated to the use of S-N curves enables to compute the damage. However, this approach leads to the same damage whatever the order of the cycles, which may lead to large approximation errors. Continuous damage approaches (Allix et al. (1989); Francfort and Marigo (1993)) offer the possibility to take into account the loading history and are more general than the ones based on empirical studies (Fatemi and Yang (1998)). In this article, we propose to used the fatigue damage Lemaitre and Doghri (1994) which considers elastic behaviour at a macroscopic scale and elastoplastic behaviour with damage evolution law at a microscopic scale to model micro-cracks caused by fatigue phenomenon. This model is briefly presented in Section 2. The objective of this article is to compare the linear damage accumulation model with the two-scale fatigue damage model in a stochastic framework. In order to perform this comparison, we first identify the random material parameters of

the two-scale fatigue domain from the random S-N curves using a Bayesian approach in Section 3. By improving the methodology proposed in Rocher et al. (2020), we obtain a better conservative approximation of the S-N curves. Then, in Section 4, the two models (linear and non-linear damage accumulation) are compared on a two-dimensional mechanical example for three different loads in terms of final damage and final probability of failure. Finally, we propose in Section 5 a strategy to build a meta-model of the damage that will be used to estimate instantaneous and final probability of failure while keeping numerical costs under control and offering a stochastic approximation of fatigue damage.

2. TWO-SCALE FATIGUE MODEL

We consider the model proposed by Lemaitre and Doghri Lemaitre and Doghri (1994). Two different scales are defined: the macroscopic scale and the microscopic scale. At the macroscopic scale the behaviour is linear isotropic elastic with Young modulus E and Poisson coefficient ν. Therefore the relation between the stress $\underline{\underline{\sigma}}$ and the small strain $\underline{\underline{\varepsilon}}$ is

$$\underline{\underline{\sigma}} = \left(\frac{E}{1-2\nu}\mathbf{P^H} + \frac{E}{1+\nu}\mathbf{P^D} \right) : \underline{\underline{\varepsilon}} \tag{1}$$

Where $\mathbf{P^H}$ and $\mathbf{P^D}$ are the hydrostatic and deviatoric projectors. Only the macroscopic scale affects the microscopic scale via the Lin-Taylor relationship: $\underline{\underline{\varepsilon}}^\mu = \underline{\underline{\varepsilon}}$ (all quantities of the microscopic scale have an exponent μ). At the microscopic scale, the behaviour is elastoplastic with damage evolution. We assume the partition of elastic and plastic strains:

$$\underline{\underline{\varepsilon}}^\mu = \underline{\underline{\varepsilon}}^{\mu e} + \underline{\underline{\varepsilon}}^{\mu p} \tag{2}$$

The elastic properties are the same at both scales so that, at the microscopic scale, the Hooke's law reads:

$$\begin{aligned} \underline{\underline{\sigma}}^\mu &= (1-D^\mu)\left(\frac{E}{1-2\nu}\mathbf{P^H} + \frac{E}{1+\nu}\mathbf{P^D} \right) : \underline{\underline{\varepsilon}}^{\mu e} \\ &= (1-D^\mu)\underline{\underline{\tilde{\sigma}}}^\mu \end{aligned} \tag{3}$$

where D^μ is the damage. We consider elasto-plasticity with kinematic hardening of modulus C and yield strength σ_y^μ and damage evolution when the cumulative plastic strain p is equal to p_D. The evolutions of plasticity and damage are given by the following equations:

$$\begin{cases} f = \sqrt{\frac{3}{2}} \| \mathbf{P^D} : \underline{\underline{\tilde{\sigma}}}^\mu - \underline{\underline{X}}^\mu \| - \sigma_y^\mu \\ d\underline{\underline{X}}^\mu = \frac{2}{3} C (1-D^\mu) d\underline{\underline{\varepsilon}}^{\mu p} \\ dp^\mu = \sqrt{\frac{2}{3}} \| d\underline{\underline{\varepsilon}}^{\mu p} \| \\ dD^\mu = \frac{1}{2S} (\underline{\underline{\tilde{\sigma}}}^\mu : \underline{\underline{\varepsilon}}^{\mu e}) dp^\mu \end{cases} \tag{4}$$

where S is a damage parameter and $\|\underline{\underline{x}}\|^2 = \sum_{i,j} x_{ij}^2$. The critical damage D_C is the upper bound of the microscopic damage D^μ. The case $D^\mu = D_C$ corresponds to the coalescence of microscopic cracks leading to macroscopic crack and to failure after few cycles.

The elastic properties are usually well-known so that we consider $E = 210$ GPa and $\nu = 0.3$ deterministic. σ_y^μ is the fatigue limit and is considered deterministic. Therefore, 4 random material parameters (S, C, D_c, and p_D) are modelled as random variable.

3. IDENTIFICATION OF RANDOM MATERIAL PARAMETERS

The objective of this subsection is to identify the distributions of the random parameters C, S, D_c and p_D from the S-N curves using Monte Carlo Markov Chain (MCMC) (Hastings (1970)) as a Bayesian calibration technique. To do this, we need:

- Observations N_{obs} for different stress amplitudes $\Delta\sigma_i$
- A priori distribution for each random variable S, C, D_c, and p_D
- A model that enables to compute the number of cycles $\hat{N}$ from S, C, D_c, and p_D
- The application of the Bayes's theorem
- The generation of a population with Metropolis-Hastings algorithm

Each of these ingredients is detailed in the following subsections.

3.1. Observations

In Det Norske Veritas (DNV (2014)) the distribution of the number of cycles to failure N for a stress range $\Delta\sigma_i$ is approximated by:

$$\log_{10}(N) = \begin{cases} a\log_{10}(\Delta\sigma_i) + \log_{10}(b) & \text{if } \Delta\sigma_i \geq 2\sigma_y^\mu \\ +\infty & \text{otherwise} \end{cases} \tag{5}$$

Where a is deterministic and b follows a log-normal law of variance 0.04. Here, we consider the case of a tubular joint whose asymptotic fatigue limit is 10^6 cycles so that $a = -3$ and $\sigma_y^\mu = 41.703$MPa. The deterministic S-N curve associated to the quantile 2.3% is obtained for a realization b of 12.164. We consider $I = 10$ stress amplitudes $\Delta\sigma_i$ in the interval $[93.4; 493.4]$MPa. At each amplitude $\Delta\sigma_i$, we generate $K = 10^4$ observations of the number of cycles $N_{obs,k}(\Delta\sigma_i)$ using (5).

3.2. A priori distributions

From literature (Lemaître (2001); Lemaître and Desmorat (2005)) and after a one at time elastic sensitivity analysis, we propose the following uniform a priori distributions for the random material parameters: $C \sim \mathscr{U}(2.10^6, 3.10^6)$ (MPa), $S \sim \mathscr{U}(10^{-3}, 1)$ (MPa), $D_c \sim \mathscr{U}(0, 0.5)$, $p_D \sim \mathscr{U}(0,1)$.

3.3. Model $\hat{N}$

We consider the two-scale damage model presented in Section 2 in a one-dimensional framework (that is to say all variables are scalar). For sinusoidal macroscopic stress centered in zero with a constant stress amplitude $\Delta\sigma_i$, we can derive the following expression of the number of cycles $\hat{N}$ for which $D = D_c$:

$$\hat{N}(\Delta\sigma_i) = \frac{2C+3E}{6(\Delta\sigma_i - 2\sigma_y^\mu)} p_D + \frac{2CES}{\left(\tilde{\sigma}_i^{\mu^3} - (2\sigma_y^\mu - \tilde{\sigma}_i^\mu)^3\right)} D_C \tag{6}$$

where $\tilde{\sigma}_i^\mu = \frac{C\Delta\sigma_i + 3E\sigma_y^\mu}{2C+3E}$ the effective stress at the microscopic scale.

3.4. Bayes's theorem

To account for both modeling and measurement errors, we introduce the error $\xi \sim \mathscr{N}(0, \mathbb{V}_\xi)$ between the model and the observations:

$$N_{obs}(\Delta\sigma_i) = \hat{N}(\Delta\sigma_i) + \xi \tag{7}$$

The variance $\mathbb{V}_\xi$ is unknown and will be identified during the MCMC algorithm. The a priori density of probability of $\mathbb{V}_\xi$ is $\mathscr{U}(0,1)$. We note φ_ξ the density probability function of ξ. We gather the 5 scalars C, S, D_C, p_D and $\mathbb{V}_\xi$ in a vector $\underline{z}$.

Bayes' theorem expresses the posterior distribution $f_{\underline{Z}}(\underline{z})$ from the prior distribution $p_{\underline{Z}}(\underline{z})$:

$$f_{\underline{Z}}(\underline{z}) = c\, p_{\underline{Z}}(\underline{z}) \mathscr{L}(\underline{z}, N_{obs}) \tag{8}$$

c is a normalization factor that can be computed at the end of the procedure easily by normalizing the a posteriori probability densities. $\mathscr{L}(\underline{z}, N_{obs})$ is the likelihood function defined as:

$$\begin{cases} \mathscr{L}(\underline{z}, N_{obs}) = \prod_{i=1}^{I} \varphi_\xi(\xi_i) \\ \xi_i = \min\limits_{k \in [\![1;K]\!]} |\log_{10}(N_{obs,k}(\Delta\sigma_i)) - \log_{10}(\hat{N}(\Delta\sigma_i))| \end{cases} \tag{9}$$

3.5. Metropolis-Hastings algorithm

The objective of the Metropolis-Hastings algorithm is to generate a population gathering q_{max} realizations of $\underline{z}$ leading to the same distribution $\hat{N}$ than N_{obs}. The principle is to generate candidates $\tilde{\underline{z}}$ using the a priori distributions and decide if they are kept in the final generated population by comparing their likelihood with the observations. The candidate is generated from the previous conserved realization by changing only one of the 5 random variables at a time. The main steps are described in Algorithm 1.

Algorithm 1: MCMC algorithm

```
Set q = 0;
Initialize z^q with the mean of the a priori
  distribution of each random variable;
Define the size of the final population q_max;
while q < q_max do
    Generate a candidate z̃ from z^q;
    Compute α = min(1, L(z̃, N_obs) / L(z^q, N_obs));
    Generate a realization β of U(0,1);
    if β < α then
        q = q + 1;
        z^{q+1} = z̃;   // candidate is kept
        Append z^{q+1} to the population ;
    end
end
```

We consider $L = 10$ sets of observations. For each of them, we perform the MCMC approach $M = 10$ times using the Algorithm 1. For each of the $L \times M$ generated populations of $\underline{Z}$, we can compute the number of cycles $\hat{N}$ and estimate the quantile 2.3%. We decide that the most accurate population is the one that both:

- minimizes the relative error with S-N curve (quantile 2.3%) built from the observations
- underestimates the number of cycles on the range $[138.1; 493.4]$MPa to obtain conservative results

The variability of the $L \times M$ populations is illustrated on Figure 1. We also give the quantile plotted from the L sets of observations (they all superimposed) and the one obtained from the chosen population. We observe that for $\Delta\sigma_i = 93.4$MPa, the error is large. This can be explained by the fact that the chosen S-N curve is bilinear, whereas the fatigue two-scale model is of class C^1 and designed only for polycyclic fatigue.

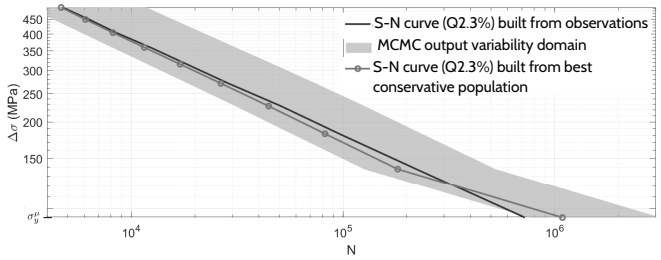

Figure 1: S-N curves (Q2.3%) computed from observations N_{obs} and from the most accurate population

3.6. Results

Once the population is selected, we can compute the means, standards deviations, correlations coefficients as well as joint and marginal distributions of S, C, D_c and p_D. They are presented in Tables 1 and 2 and Figure 2.

We observe that only D_C and S are correlated. The obtained distribution of C and p_D are both uniform.

	C (MPa)	S (MPa)	D_C	p_D
Mean	$2.507\ 10^6$	0.612	0.303	0.554
std	$2.900\ 10^5$	0.2313	0.116	0.260

Table 1: Means and standard deviations (std)

R	C (MPa)	S (MPa)	D_C	p_D
C (MPa)	1	−0.058	−0.039	0.003
S (MPa)	−0.058	1	−0.260	−0.022
D_C	−0.039	−0.260	1	−0.019
p_D	0.003	−0.022	−0.019	1

Table 2: Bravais-Pearson correlation coefficients

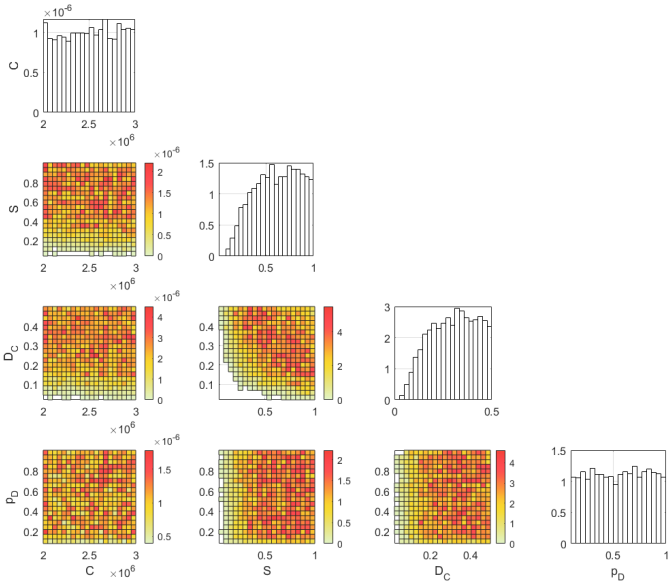

Figure 2: Joint and marginal distributions of $\boldsymbol{Z}$

4. Comparison between linear and nonlinear damage accumulation

In this section, we compare the damage computed with the two-scale fatigue model presented in Section 2 which accounts for loading history, with the damage obtained with the standard Rainflow counting and Palmgreen and Miner linear damage accumulation. In the first subsection, we present the case study. In the second subsection, we define the three loads considered. In the third subsection, we explain the computation of the damage for both models. In the fourth subsection, we give the results.

4.1. Description of the structure

We consider a rectangular structure clamped on the left-hand side. A sollicitation $F(t)$ with $t \in [0;t_{end}]$ is imposed on the right-hand side. The structure is meshed with linear quadrangular elements and only one element is damageable (in black in Figure 3, bottom-left). We assume plane stress. The deterministic parameters are $E =$ 210GPa, $\nu = 0.3$, $\sigma_y^{\mu} = 41.703$MPa.

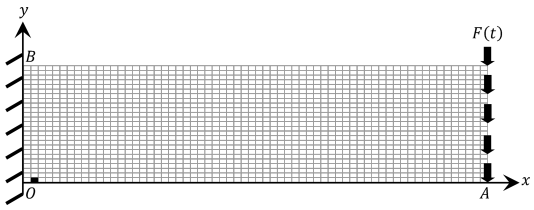

Figure 3: Meshed structure with boundary conditions and damageable element

4.2. Definition of the loads

We define 3 three loads $F_1(t)$, $F_2(t)$ and $F_3(t)$ with growing complexity that lead to equivalent number of cycles and equivalent damage at $t = t_{end}$ with linear damage accumulation. All loads are centered in 0. The first load $F_1(t)$ is centered on 0 generating a local constant stress amplitude $\Delta\sigma_1$ such that there are n^* cycles in the time interval $[0;t_{end}]$. The final damage is $D^* = \frac{n^*}{N(\Delta\sigma_1)}$. The second signal $F_2(t)$ is a realization of a Gaussian process with Gaussian correlation. The variance, expected value and correlation lengths are chosen such that the number of cycles is n^* and the final damage is D^*. The third load $F_3(t)$ is the same as $F_2(t)$ but with Matern correlation.

We give truncated series of the three local stresses associated to the three loads in Figure 4.

4.3. Computation of damage

In the case of linear accumulation fatigue model, the material uncertainty comes from the random variable b in (5). Thus, 5000 realizations b are generated and the damage is computed with Palmgreen and Miner's rule (Miner (2021)):

$$D(t_{end}) = \sum_{q}^{cycles} \frac{n(\Delta\sigma_q)}{b\Delta\sigma_q^a} \tag{10}$$

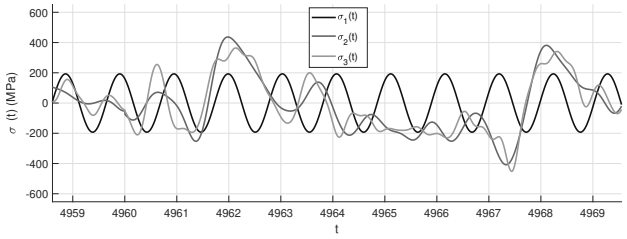

Figure 4: Truncated series of the local stresses associated to the three loads

where $n(\Delta\sigma_q)$ is the number of cycles of amplitude $\Delta\sigma_q$ that can be obtained by Rainflow counting (Hong (1991)). Failure occurs when $D = 1$.

In the case of the non-linear accumulation fatigue model, a sample of 5000 realizations of the material parameters C, S, p_D and D_C is generated from the distributions identified in subsection 3. Then, a radial return algorithm with time step $\delta t = 0.005$ is used to compute the evolution of plasticity in damage, following equations presented in subsection 2. Failure occurs when $D = D_C$.

4.4. Comparison of final damage

In Tables 3 and 4, we give the number of trajectories leading to failure and the probability of failure at $t = t_{end}$ for both models.

	F_1	F_2	F_3
non-linear accumulation	166	206	662
linear accumulation	109	109	263

Table 3: Number of failed realizations at $t = t_{end}$

	F_1	F_2	F_3
non-linear accumulation	3.5	4.3	13.1
linear accumulation	2.3	2.3	5.5

Table 4: Probability of failure (%) at $t = t_{end}$

We observe that linear damage accumulation give equivalent results for loads 1 and 2. This is expected as the second load has been defined to obtain the same final damage as the first load. Note that the Maters correlation introduces more cycles which doubles the number of trajectories leading to failure. Moreover, for the second load, the non-linear damage accumulation leads final probability

of failure twice as large as the linear accumulation model. The difference is even more significant for the third load with a factor of almost 3 between the two models. This clearly shows that it is crucial to take into account the loading history. We also give the total computational time required to obtain the probability of failure at $t = t_{end}$ in Table 5. As expected, that the linear accumulation is far cheaper than the non-linear accumulation.

	F_1	F_2	F_3
non-linear accumulation	167	167	167
linear accumulation	1.39	1.39	1.39

Table 5: Computational time (hours)

It is then interesting to perform a time variant sensitivity analysis using Borgonovo's method Pianosi et al. (2014). The time variant sensitivity index $\delta(D^\mu(t), Z_j)$ of $D^\mu(t)$ with respect of Z_j is then written:

$$\delta = \frac{1}{2}\int_{Z_{j_{\min}}}^{Z_{j\max}} f_{Z_j}(z_j) \int_{D_{C_{\min}}}^{D_{C\max}} \left| f_{D^\mu(t)}(D^\mu(t)) - f_{D^\mu(t)|Z_j}(D^\mu(t)|z_j) \right| dD^\mu(t) dz_j \tag{11}$$

where f_{Z_j} and $f_{D^\mu(t)}$ are the probability distribution functions of Z_j and $D^\mu(t)$, respectively. In Figure 5, we give the time variant sensitivity indexes of the damage $\delta(D^\mu)$ with respect to each of the random material parameters.

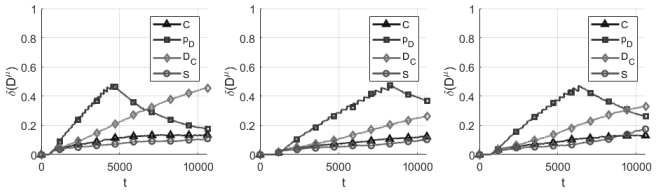

Figure 5: Sensitivity for loads 1 (left), 2 (center) and 3 (right)

We observe that the damage is weakly sensitive to S and C. On the contrary, the sensitivity index of D^μ with respect to p_D increases with time before decreasing. Indeed, p_D only affects the beginning of the damage evolution as it is the threshold for damage initiation. The sensitivity index of D^μ with respect to D_C increases with time because D_C is only used in the model as the maximum critical value of D^μ. Once, $D^\mu = D_c$, the damage is constant, failure occurs and the computation is stopped.

5. META-MODELLING OF DAMAGE EVOLUTION

The comparison done in subsection 4.4 shows that taking into account loading history is crucial for fatigue damage prediction. The two-scale model is incremental and both material parameters and loading are random. As a consequence, the estimation of the instantaneous probability of failure $P_f(t) = \text{Prob}(D_c \leq D^\mu(t))$ using crude Monte Carlo estimation is impossible due to prohibitive computational costs. Therefore, we propose to build a multi-fidelity kriging-based meta-model of the damage D^μ from observations on two levels: the first (cheap coarse) level is the linear damage accumulation (equation 10) and the second (accurate expensive) level is the two-scale non linear cumulative damage (presented in Section 2).

5.1. Brief description of kriging meta-modelization

Let consider that m observations (or computations) at $\underline{x}_1^{obs} \dots \underline{x}_m^{obs}$ of a model g are gathered in a vector of observations $\underline{g}^{obs}$. Kriging (Krige (1951)) relies on the hypothesis that the objective function g is the realization of a stationary Gaussian process G

$$G(\underline{x}) = y(\underline{x}) + Z(\underline{x}) \tag{12}$$

where $\underline{x} \in \mathbb{R}^d$, $y(\underline{x})$ is the mean of $G(\underline{x})$ and $Z(\underline{x})$ is a random variable distributed as a centered Gaussian. Here, we consider ordinary kriging so that $y(x) = \beta$ where β is an unknown constant. The estimation $\hat{g}$ of g is chosen as a linear combination of observations: $\hat{g}(\underline{x}) = \underline{w}(\underline{x})^T \underline{g}^{obs}$, where $\underline{w}(\underline{x})$ are the kriging coefficients to be determined.

$\hat{g}$ is searched as the best linear unbiased predictor, which reads :

$$\begin{cases} \mathbb{E}\left[\hat{g} - G\right] = 0 \\ \beta = \arg\min \mathbb{E}\left[(\hat{g} - G)^2\right] \end{cases} \tag{13}$$

where $\mathbb{E}$ is the expectation.

Before solving system (13) the covariance matrix of the data has to be computed. In this paper, we use a Matern-correlation function which introduces the following hyperparameters: the variance s^2 and the correlation lengths $\underline{\theta} = [\theta_1, \dots, \theta_d]$. Several techniques exist to estimate them. Here we use

the maximum likelyhood estimation (Wasserman, 2013, p. 124). Once the hyperparameters are determined, the optimization system (13) is solved: the meta-model is built.

5.2. *Construction of the multi-fidelity meta-model*

To ease the illustrations, we choose to fix $C = 2.10^6$MPa, $S = 0.3$MPa, D_c=0.4. p_D is the only material random variable following uniform distribution between 0 and 1, as identified in subsection 3.6. The meta-models are functions of the time t and of p_D. Following the standard auto-regressive cokriging approach (Kennedy and O'Hagan (2000)) the multi-fidelity meta-model reads:

$$\hat{D}^{\mu}(t,p_D) = \rho\hat{D}(t,p_D) + \hat{z}(t,p_D) \qquad (14)$$

$\hat{D}(t,p_D)$ is the meta-model built from r evaluations $D(t_i,p_{D,i})$ of the linear cumulative damage on r observation points $(t_i,p_{D,i})_{i=1..r}$. $\hat{z}(t,p_D)$ is the meta-model of the error between the two levels built from the observed error $z(t_i,p_{D,i}) = D^{\mu}(t_i,p_{D,i}) - D(t_i,p_{D,i})$ on q observations points $(t_i,p_{D,i})_{i=1..q}$. The objective is to choose $q << r$ as the computation of the error z is more expensive than the computation of D. The q observations points are included in the r observations points at the coarse level. ρ is an additional hyperparameter due to the use of different levels. The multi-fidelity meta-model is obtained by doing the sum described in Equation (14).

5.3. *Results*

We illustrate the strategy on the study case of the plate with the third load. $r = 80$ observations points are generated thanks to Latin Hypercube Sampling (LHS). Among those points, $q = 16$ are chosen with LHS. The two kriging-based meta-models are built with anisotropic Matern-3/2 kernel and hyperparatemers (ρ and correlation lengths) are computed using the likelyhood function.

In Figure 5.3, we give the meta-modelization $\hat{D}(t)$, the multi-fidelity meta-modelization $\hat{D}^{\mu}(t,p_D)$ and the reference damage $D^{\mu}(t,p_d)$ computed with the non-linear cumulative damage.

We observe that the multi-fidelity meta-model $\hat{D}^{\mu}$ is a very good approximation of $D^{\mu}(t,p_D)$. We notice that the meta-model leads to non monotonic

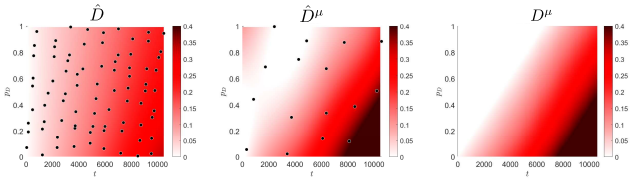

Figure 6: Meta-models and reference damage : black dots are the observations

damage. This can be partially solved by using more observations points without re running computations. Indeed, as the two-scale model is incremtal, if $D(t_i,p_{D,i})$ is known, $\forall t \in [0;t_i]$, $D(t,p_{D,i}$ is also known.

In Table 6, we give the probability of failure at $t = t_{end}$ computed from the multi-fidelity meta-model $\hat{D}^{\mu}$, the low mono-fidelity meta-model $\hat{D}$, the reference D^{μ}. Only 16 evaluationw of the two-scale damage model are realized. The three probabilities of failure are computed by Monte Carlo estimation on a population of 10^3 realizations of p_D.

$P_f(t_{end})$ computed with $\hat{D}^{\mu}$	0.449
$P_f(t_{end})$ computed with $\hat{D}$	0.000
$P_f(t_{end})$ computed with D^{μ}	0.469

Table 6: Final probability of failure obtained with the meta-models and with the reference

Note that the reference probability of failure 0.469 is different from the one obtained in subsection 4.4 where all material parameters were random. Using linear cumulative damage, the final probability of failure is 0. This was expected as Figure shows that $\hat{D}$ never exceeds $0.35 < D_C$. The probability of failure estimated with the multi-fidelity meta-model is very close to the one obtained with the reference (relative error about 5%).

Finally, in Table 7, we give the total computational time required to estimate the probability of failure at $t = t_{end}$ with the multi-fidelity meta-model $\hat{D}^{\mu}$, the low mono-fidelity meta-model $\hat{D}$ and the reference D^{μ}.

We observe that the total computational time to compute $P_f(t_{end})$ is very close to the computational time necessary to realize the observations (calls to the model). The construction of the meta-model

Using $\hat{D}^{\mu}$	400
Using $\hat{D}$	80
Using D^{μ}	20 000

Table 7: Total computational time required for the esimation fo $P_f(t_{end})$ (minutes)

are the Monte Carlo estimation are negligible. We observe that the multi-fidelity meta-model offers a speed up of 50 compared to the reference.

6. CONCLUSIONS

In this article, we used a continuous damage model in a stochastic framework to assess the fatigue lifetime of structure. After a Bayesian calibration of the random material parameters from S-N curves, we observe that taking into account the loading history is crucial to accurately estimate the final damage in case of complex loads. Moreover, the time variant sensitivity analysis enables to understand the role of each material random variable of the two-scale fatigue model. Finally, in a first application, we built a multi-fidelity meta-model from cheap computations with linear damage accumulation model and a few expensive computations on the expensive two-scale fatigue model. The exploitation of this meta-model show its ability to control numerical cost on the estimation of the probability of failure. Future works will consist in developing the metamodeling strategy of damage by studying the enrichment procedure, include all random material parameters and take advantage from the knowledge obtained with the sensibility analysis to optimize the computational costs.

7. REFERENCES

Allix, O., Ladevèze, P., Gilletta, D., and Ohayon, R. (1989). "A damage prediction method for composite structures." *International Journal for Numerical Methods in Engineering*, 27, 271–283.

DNV (2014). "RP-C203: Fatigue of offshore steel structures.

Fatemi, A. and Yang, L. (1998). "Cumulative fatigue damage and life prediction theories: a survey of the state of the art for homogeneous materials." *International Journal of Fatigue*, 20(1), 9–34.

Francfort, G. A. and Marigo, J.-J. (1993). "Stable damage evolution in a brittle continuous medium." *European Journal of Mechanics A-solids*, 12, 149–189.

Hastings, W. K. (1970). "Monte carlo sampling methods using markov chains and their applications." *Biometrika*, 57, 97–109.

Hong, N. (1991). "A modified rainflow counting method." *International Journal of Fatigue*, 13(6), 465–469.

Kennedy, M. and O'Hagan, A. (2000). "Predicting the output from a complex computer code when fast approximations are available." *Biometrika*, 87(1), 1–13.

Krige, D. (1951). "A statistical approach to some basic mine valuation problems on the witwatersrand." *Journal of the Southern African Institute of Mining and Metallurgy*, 52(6), 119–139.

Lemaître, J. (2001). "Handbook of materials behavior models.

Lemaître, J. and Desmorat, R. (2005). "Engineering damage mechanics: Ductile, creep, fatigue and brittle failures.

Lemaitre, J. and Doghri, I. (1994). "Damage 90: a post processor for crack initiation." *Computer Methods in Applied Mechanics and Engineering*, 115(3), 197–232.

Miner, M. A. (2021). "Cumulative damage in fatigue." *Journal of Applied Mechanics*, 12(3), A159–A164.

Pianosi, F., Beven, K. J., Freer, J. E., Hall, J. W., Rougier, J., Stephenson, D. B., and Wagener, T. (2014). "Sensitivity analysis of environmental models: A systematic review with practical workflow." *Environ. Model. Softw.*, 79, 214–232.

Rocher, B., Schoefs, F., François, M., Salou, A., and Caouissin, A.-L. (2020). "A two-scale probabilistic time-dependent fatigue model for offshore steel wind turbines." *International Journal of Fatigue*, 136, 105620.

Wasserman, L. (2013). *All of statistics: a concise course in statistical inference*. Springer Science & Business Media.